Supporting Information

Suh et al. 10.1073/pnas.1108269108

SI Materials and Methods

Generation of Neph-B1 Transgenic Mice. The mouse and human *LAMB1* cDNAs were digested with SphI and ligated to make a full-length mouse/human chimeric cDNA. This chimeric cDNA was placed under the control of the 4.1-kb Nephrin promoter, and SV40 3′ processing signals were added. This Neph-B1 construct was purified away from plasmid vector sequences and injected into the pronuclei of single-celled B6CBAF2/J mouse embryos. Transgenic founders were identified by PCR genotyping and bred to generate lines. Expression was assayed by immunostaining sections of postnatal kidney with a monoclonal antibody to the C terminus of human Lamβ1. Primers used for genotyping of Neph-B1 transgenic mice were 5′-gga cag aaa gac tgc gac agt cac aga caa-3′ and 5′-caa agg cga aca cct gga gca gcc cca tgt-3′.

Antibodies. Antibodies used for immunostaining were: rabbit antimouse laminin β2 and rabbit antimouse laminin β1 (1), rat antimouse laminin α1 mAb 8B3 (2), mouse antihuman laminin β1 mAb 3E5 (Millipore), mouse antihuman desmin mAb D33 (Dako), rabbit antipodocin (3), rabbit antimouse laminin α5 (8948) (4), rat antimouse laminin α2 mAb 4H8 (ALEXIS Biochemicals/Axxora) (5), rabbit antihuman laminin-332 (6), Alexa Fluor-594–conjugated antimouse IgG1 and antimouse IgG2a (Molecular Probes), FITC-conjugated antirat and antirabbit, and Cy3-conjugated antirat and antirabbit (Chemicon).

1. Sasaki T, Mann K, Miner JH, Miosge N, Timpl R (2002) Domain IV of mouse laminin beta1 and beta2 chains. *Eur J Biochem* 269:431–442.
2. Abrahamson DR, et al. (1989) Selective immunoreactivities of kidney basement membranes to monoclonal antibodies against laminin: Localization of the end of the long arm and the short arms to discrete microdomains. *J Cell Biol* 109:3477–3491.
3. Roselli S, et al. (2002) Podocin localizes in the kidney to the slit diaphragm area. *Am J Pathol* 160:131–139.
4. Miner JH, et al. (1997) The laminin alpha chains: Expression, developmental transitions, and chromosomal locations of alpha1-5, identification of heterotrimeric laminins 8-11, and cloning of a novel alpha3 isoform. *J Cell Biol* 137:685–701.
5. Schuler F, Sorokin LM (1995) Expression of laminin isoforms in mouse myogenic cells in vitro and in vivo. *J Cell Sci* 108:3795–3805.
6. Marinkovich MP, Lunstrum GP, Keene DR, Burgeson RE (1992) The dermal-epidermal junction of human skin contains a novel laminin variant. *J Cell Biol* 119:695–703.

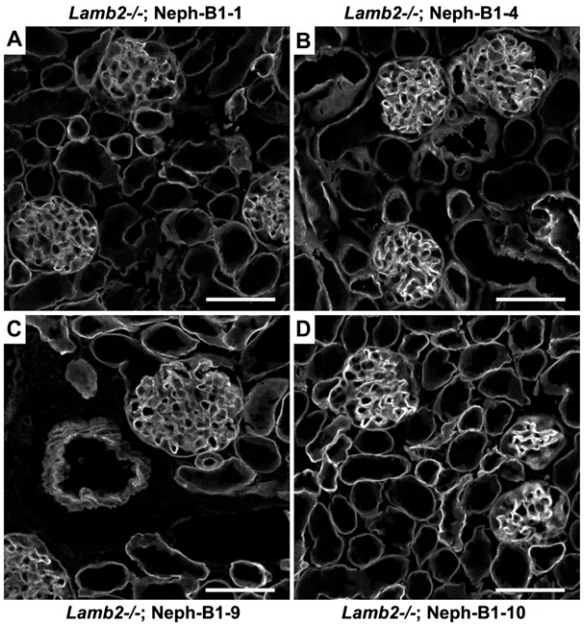

Fig. S1. Confocal immunofluorescence analysis of Lamβ1 transgene expression in four different lines. All transgenic lines showed linear GBM staining for Lamβ1, although the level varied among the lines. The different lines were divided into two groups, low (*A*) and high (*B*–*D*) expressors. (Scale bars, 50 μm.)

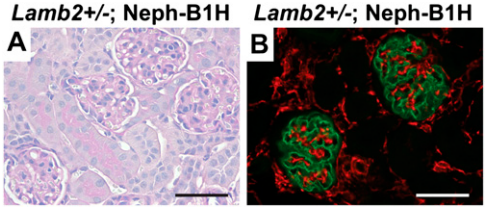

Fig. S2. Three-wk-old *Lamb2* heterozygous mice with transgene show normal glomerular histology. (*A*) PAS staining. (*B*) Immunofluorescence analysis of podocin (green) and desmin (red). Lamβ1 transgene expression did not affect podocyte integrity or glomerular architecture. (Scale bars, 50 μm.)

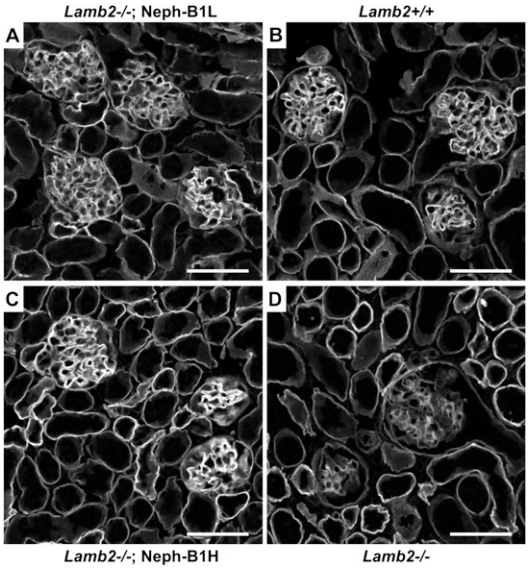

Fig. S3. Confocal immunofluorescence analysis of laminin α5 in the GBM. (*A* and *C*) Lamα5 deposition in the GBM of *Lamb2*$^{-/-}$; Neph-B1 mice (*A*, low expressor; *C*, high expressor) was increased by Lamβ1 expression in podocytes. Note that higher Lamβ1 expression was accompanied by higher Lamα5 in the GBM, presumably as part of the LM-511 trimer. (*B* and *D*) Lamα5 shows a linear deposition in the wild-type GBM (*B*), whereas Lamα5 is significantly reduced in the *Lamb2*$^{-/-}$ GBM (*D*). Quantified results are in Fig. 5*J*. (Scale bars, 50 μm.)

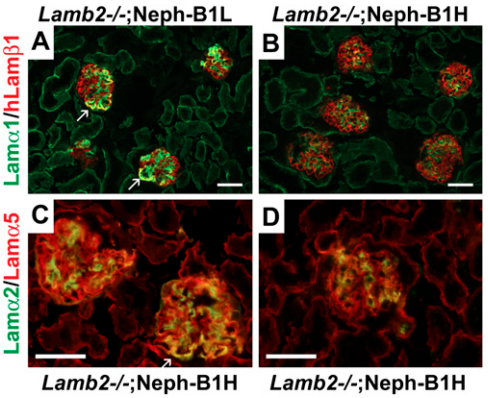

Fig. S4. Ectopic deposition of Lamα1 and Lamα2 in the GBM of 1-y-old *Lamb2*$^{-/-}$; Neph-B1 mice. Immunofluorescence analysis of GBM deposition of (*A* and *B*) Lamα1 (green) and transgenic Lamβ1 (red); and (*C* and *D*) Lamα2 (green) and Lamα5 (red). Note that some transgenic mice did not show ectopic deposition of Lamα1 and Lamα2 in the GBM (*B* and *D*). (Scale bars, 50 μm.)

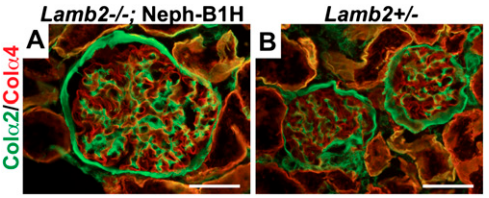

Fig. S5. The deposition of type IV collagen was not affected by Neph-B1 transgene expression. (*A* and *B*) Immunofluorescence analysis shows that collagen α2 (IV) [green; represents the α1α1α2(IV) network] was deposited in the mesangial matrix and collagen α4(IV) [red; represents the α3α4α5(IV) network] was deposited in the GBM, regardless of the expression of the Lamβ1 transgene (*A*, with Lamβ1 transgene; *B*, without Lamβ1 transgene). (Scale bars, 50 μm.)

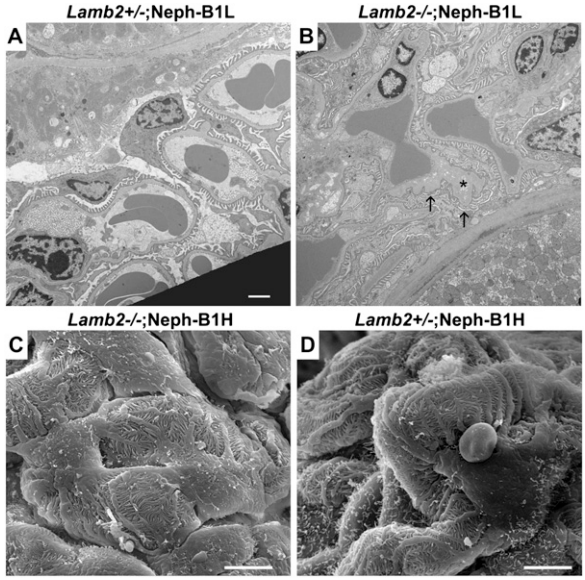

Fig. S6. Ultrastructural analysis of glomeruli. (*A* and *B*) Transmission electron micrographs of glomerular capillary loops from 1-y-old mice. Note that the segmental thickening of the GBM (arrows) in *Lamb2*$^{-/-}$; Neph-B1 mice was observed without severe podocyte foot process effacement. Asterisk indicates electron lucent areas in the expanded lamina densa. (*C* and *D*) Scanning electron micrographs of glomeruli from 1-y-old mice. There was not much difference in the extent of foot process integrity between *Lamb2*$^{-/-}$; Neph-B1 and control. [Scale bars, 2 μm (*A* and *B*) and 5 μm (*C* and *D*).]